Biol. Cybern. 86, 263–270 (2002)
DOI 10.1007/s00422-001-0296-8

Biological Cybernetics

Pathological tremors as diffusional processes

J. B. Gao[1], **Wen-wen Tung**[2]

[1] Electrical Engineering Department, University of California, Los Angeles, CA 90095, USA
[2] Department of Atmospheric Sciences, University of California, Los Angeles, CA 90095, USA

Received: 30 May 2001 / Accepted in revised form: 6 November 2001

Abstract. Two types of pathological tremors, essential and Parkinsonian, are studied using dynamical systems theory. It is shown that pathological tremors can be characterized as diffusional processes. The time-scale range for the diffusional scaling law to be valid starts from about one to several tens of the mean oscillation period. This time-scale range contrasts sharply with the predictable time scale for deterministic chaos, which is usually only a small fraction of the mean oscillation period. The diffusions in pathological tremors are usually anomalous. A number of quantities are designed to characterize the diffusions in the tremor. Their relevance to potential clinical applications is discussed. It is argued that in order to discriminate between Parkinsonian and essential tremors, quantities not of purely dynamical origin may be more useful, since purely dynamical quantities emphasize more the dynamical similarities between the two types of tremors.

1 Introduction

Tremor denotes an involuntary, approximately rhythmic, and roughly sinusoidal movement of parts of the body (Elble and Koller 1990). Broadly speaking, there are two classes of tremors: normal and pathological. The latter of course also contains many different types such as task- and position-specific tremors, and Holmes' tremor. For a classification of tremors based on clinical assessment, we refer to Deuschl et al. (1998).

Pathological tremors result from disorders of the central nervous system and peripheral nervous system (see Bock and Wenderoth 1999; Wenderoth and Bock 1999; and references therein). Among the many types of pathological tremors, the two most common are essential and Parkinsonian tremors. Usually, they exhibit a nonlinear oscillation. The oscillation is, however, only roughly periodic. While the frequency of the oscillation is relatively fixed, the amplitude and shape of tremor can have wide fluctuations (Gresty and Buckwell 1990). Using a number of techniques from nonlinear dynamics theory, including analyses of Lyapunov exponents, deterministic versus stochastic plots, and the $\delta-\epsilon$ method, Timmer et al. (2000) carefully studied several high-quality essential and Parkinsonian tremor data. They suggest that the deviation from periodicity is not due to deterministic chaotic dynamics; rather, it is due to nonlinear stochastic dynamics. By studying the stochastically driven van der Pol oscillator, they further suggest that second-order stochastic processes may be sufficient for the modeling of essential and Parkinsonian tremors. While their claim that dynamic noise is an important element of pathological tremor dynamics is persuasive, a number of questions remain to be answered. In light of dynamical systems theory, one of the most important questions is: Does any scaling law exist for pathological tremors?

An important feature of the stochastically driven van der Pol oscillator is that phase points near the underlying deterministic limit cycle execute a Brownian motion-like diffusional process (Gao 1997). Hence, we specifically ask: Can pathological tremors also be described as certain type of diffusional processes? If the answer is yes, we can further ask: In terms of scaling laws, are these diffusional processes of the same nature among different types of pathological tremors, and are they similar to that of the stochastic van der Pol oscillator?

Another important question to be answered is how complex the tremor dynamics is. Along this line, one can ask if chaos is relevant to the dynamics of pathological tremors. A formal description of the problem is as follows. Suppose a pathological tremor can be described by an equation

$$\frac{\mathrm{d}\boldsymbol{x}}{\mathrm{d}t} = \boldsymbol{f}(\boldsymbol{x}, \boldsymbol{p}) + \boldsymbol{\eta}(t) \ , \tag{1}$$

Correspondence to: J.B. Gao
(e-mail: jbgao@ee.ucla.edu)

where $\boldsymbol{x}$ denotes an n-dimensional state vector, $\boldsymbol{p}$ denotes an s-dimensional parameter vector, and $\boldsymbol{\eta}(t)$ represents the stochastic forcing. We ask: Can the (unrealistic) clean system (corresponding to $\boldsymbol{\eta}(t) = \boldsymbol{0}$) be chaotic? If the answer is no, then we can be satisfied that the dynamics underlying pathological tremors is indeed simple. Note that a definitive answer to this question is not easy to obtain, since deterministic chaotic signals generated from certain chaotic attractors such as the Rossler attractor (Rossler 1976) may contain sharp spectral peaks.

The rest of the paper is organized as follows. In Sect. 2, we briefly describe the tremor data used in the paper. In Sect. 3, we describe the methodology for and the results of the analyses of pathological tremors studied here. Conclusions and discussions are in Sect. 4.

2 Data

We analyze the same pathological tremor data sets as those studied by Timmer et al. (2000). The data are available at http://phyq5.physik.uni-freiburg.de/~jeti/path_tremor. There are ten data sets altogether: five each for essential tremor and parkinsonian tremor. They are denoted as et01.dat, et02.dat,..., park01.dat, etc. These data are recordings of the acceleration of the hand measured by piezoresistive accelerometers attached to the dorsum of the out-stretched hand. For convenience, the data were normalized to zero mean and unit variance by Timmer et al. (2000), thus the unit for the data is not readily obtainable. The sampling rate for et01.dat is 300 Hz, while it is 1000 Hz for other nine data sets. There are 10240 points for et01.dat, and 30000 points for all other data sets. The et05.dat and park01.dat data sets have been analyzed in Timmer et al. (2000), where a short segment of these two data sets, together with their spectra, can be found. To better appreciate the wide variations of the amplitude of the data, we have plotted in Fig. 1 the whole time series of et05.dat. This figure will help us define the fluctuation of the amplitude later.

To compare the pathological tremor time series with the stochastically driven van der Pol oscillator, we also study the latter. It is described by

$$\begin{aligned} \mathrm{d}x/\mathrm{d}t &= y + D_1\eta_1(t), \\ \mathrm{d}y/\mathrm{d}t &= -(x^2-1)y - x + D_2\eta_2(t)\ , \end{aligned} \tag{2}$$

with $\langle \eta_i(t) \rangle = 0$, $\langle \eta_i(t)\eta_j(t') \rangle = \delta_{ij}\delta(t-t')$, $i,j = 1,2$. We have simply employed an Euler scheme. When $D_1 = D_2 = 0$ (i.e., the system is deterministic), the Euler scheme has an error $O(\delta t^2)$, where δt is the integration time step. Due to noise, we have additional terms $\delta t^{i/2}\eta_{1,2}(t)$, $i = 1,2,3,\ldots$. To ensure that the numerical scheme adopted is consistent and the error is $O(\delta t^2)$, we keep three terms involving the dynamic noise: $\delta t^{i/2}\eta_{1,2}(t)$, $i = 1,2,3$. For more details, we refer to Mannella and Palleschi (1989). Note that in Timmer et al. (2000) D_1 is set to zero, and only one term involving the dynamic noise, $\delta t^{1/2}\eta_2(t)$, is included.

3 Analyses of pathological tremors

We analyze the pathological tremor data by computing the so-called time-dependent exponent $\Lambda(k)$ curves (Gao and Zheng 1993, 1994a,b) and logarithmic displacement curves (Gao 1997). The methods have recently been successfully used to study the effects of spontaneous emission noise on the nonlinear dynamics of an optically injected semiconductor laser (Gao et al. 1999a) and noise-induced chaos (Gao et al. 1999b; Hwang et al. 2000). For a recent review, we refer to Gao et al. (1999c). To make this paper self-contained, we briefly describe the computational procedure.

Given a scalar time series, $x(1), x(2), \ldots, x(N)$, we first use the time-delay embedding technique (Packard et al. 1980; Takens 1981) to construct the vectors of the form: $X_i = (x(i), x(i+L), \ldots, x(i+(m-1)L))$, with m being the embedding dimension and L the delay time. Figure 2 shows a 2-D phase diagram for et05.dat. Similar phase diagrams can also be found in Timmer et al. (2000) and Gao et al. (1999). For convenience of defining a geometrical quantity (e.g., the diffusion width, which will be described later), we have schematically plotted a narrow box in dashed lines in the figure. For the analysis of purely chaotic signals, m and L have to be chosen properly. This is the issue of optimal embedding (see Gao and Zheng 1993, 1994b; and references therein). Mathematically speaking, optimal embedding is not

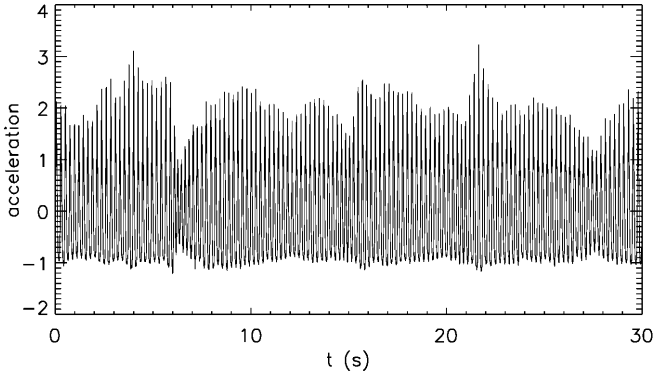

Fig. 1. The entire time series of data set et05.dat

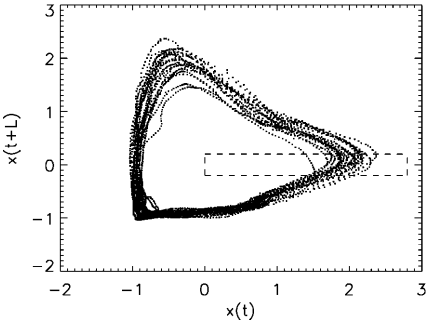

Fig. 2. Phase diagram for et05.dat. In units of the sampling points, $L = 50$. A squeezed box is also shown by the *dashed lines*

Table 1. Shown are various parameters for the essential tremor data. T is the period, in units of sampling points; L is the delay time for constructing the embedding space, also in units of sampling points. α_1 denotes the first diffusion exponent, while *Interval_1* denotes the corresponding scaling region. When the second scaling region exists, the diffusion exponent and its scaling region are denoted by α_2 and *Interval_2*, respectively. $DIFFU_{width}$ denotes the width of the diffusion, while AMP_{fluc} denotes the fluctuation of the amplitude

Data	et01	et02	et03	et04	et05
T	54	231	186	185	233
L	13	57	50	40	50
L/T	0.241	0.247	0.269	0.216	0.215
α_1	0.63 ± 0.005	0.63 ± 0.013	0.41 ± 0.004	0.60 ± 0.007	0.72 ± 0.004
Interval_1	1.1–8.0T	0.6–2.6T	1.1–7.4T	0.65–6.0T	1.0–9.1T
α_2			0.59 ± 0.003		
Interval_2			10.3–31.6T		
$DIFFU_{width}$	0.19	0.09	0.11	0.44	0.20
AMP_{fluc}	0.17	0.09	0.11	0.34	0.19

Table 2. Same as in Table 1, except now for the Parkinsonian tremor data

Data	park01	park02	park03	park04	park05
T	216	213	216	219	222
L	46	44	44	44	48
L/T	0.213	0.216	0.207	0.204	0.201
α_1	0.65 ± 0.005	0.53 ± 0.007	0.64 ± 0.01	0.49 ± 0.003	0.38 ± 0.008
Interval_1	1.0–10.0T	1.1–5.5T	1.1–3.5T	1.0–10.0T	1.4–8.1T
α_2		0.56 ± 0.008		0.80 ± 0.01	0.65 ± 0.01
Interval_2		9.3–17.0T		14.0–25.1T	9.9–20.3T
$DIFFU_{width}$	0.33	0.32	0.17	0.11	0.09
AMP_{fluc}	0.30	0.25	0.17	0.10	0.09

defined for the analysis of noisy data, since noisy data is infinite-dimensional. For this reason, we have more or less arbitrarily chosen $m = 4$ for this study. We have happily found, though, that the optimal delay parameter obtained by the method of Gao and Zheng (1993, 1994b) is also optimal for the study of diffusional processes, in the sense that the error for the diffusion exponent is minimal. In Tables 1 and 2 we have shown the optimal L (in units of the sampling points) for all the data sets. To make comparison of L with the (mean) periods of the tremor data, we have also included the latter in Tables 1 and 2. Note that in Timmer et al. (2000), $L = 52$ was used for et05.dat, while $L = 54$ was used for park01.dat. Hence, the L value for et05.dat in this study is quite close to that used in Timmer et al. (2000), while that for park01.dat is considerably smaller than that in Timmer et al. (2000). To check whether the ratio, L/T, could be of clinical importance, we have simply computed this ratio and included it in Tables 1 and 2. Very interestingly, we note that L/T for Parkinsonian tremor is typically smaller than that for essential tremor. Hence, this quantity might indeed be useful for discriminating between essential and Parkinsonian tremors. To establish or falsify this idea, a much larger clinical dataset would be needed.

The time-dependent exponent $\Lambda(k)$ curves are defined as (Gao and Zheng 1993, 1994a,b):

$$\Lambda(k) = \left\langle \ln\left(\frac{\|X_{i+k} - X_{j+k}\|}{\|X_i - X_j\|}\right)\right\rangle \tag{3}$$

with $r \le \|X_i - X_j\| \le r + \Delta r$, where r and Δr are prescribed small distances. The angle brackets denote ensemble averages of all possible pairs of (X_i, X_j). The integer k, called the evolution time, corresponds to time $k\delta t$, where δt is the sampling time. Geometrically $(r, r + \Delta r)$ defines a shell, and a shell captures the notion of scale. Computations are typically carried out for a series of shells. One may wonder that it might be easier to simply compute $\Lambda(k)$ for $\|X_i - X_j\| \le r$. Such (and similar) approaches were indeed proposed by Rosenstein et al. (1993) and Kantz (1994). To study the effects of both measurement and dynamic noise on chaotic systems, shells are superior to balls, because noise typically affects the small-scale dynamics more than the large-scale dynamics. For more details of these distinctions, we refer to Gao et al. (1999c).

For clean, chaotic systems, the $\Lambda(k)$ curves first increase linearly with k until some predictable time scale, k_p, (which corresponds to exponential divergence between nearby trajectories), then flattens (which corresponds to the divergence between nearby trajectories reaching the whole attractor) (Gao 1997). When the mean period of motion, T, can be defined, on average, folding has to have occurred at least once during one cycle of the motion, hence k_p is typically only a small fraction of T. The linearly increasing parts of the $\Lambda(k)$ curves corresponding to different shells collapse together to form an envelope. This property forms a direct dynamical test for deterministic chaos (Gao and Zheng 1994a,b), and enables an objective estimation of the

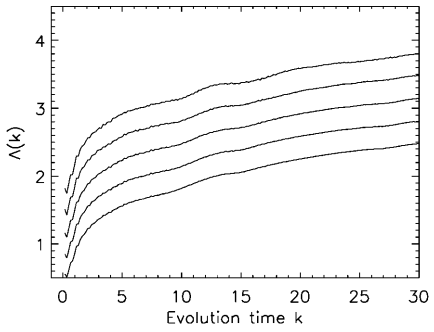

Fig. 3. Time-dependent exponent $\Lambda(k)$ vs evolution time k curves for et03.dat, where k is in units of the mean period of the motion. The five curves, from *bottom* to *top*, correspond to shells $(2^{-(i+1)/2}, 2^{-i/2})$ with $i = 8$, 9, 10, 11, and 12. The embedding parameters are $m = 4$ and $L = 50$

largest positive Lyapunov exponent (Gao et al. 1999c). When the system is corrupted by either measurement or dynamic noise, the linearly increasing parts of the $\Lambda(k)$ curves corresponding to small shells break themselves away from the envelope. However, the flat part of the $\Lambda(k)$ curves corresponding to $k > k_p$ is not altered by either measurement or dynamic noise. The flatness of the $\Lambda(k)$ curves for large k manifests the stableness of the structure of a true chaotic attractor. This property forms a necessary condition for us to assess whether the clean pathological tremor dynamics is chaotic or not. Figure 3 shows an example of the $\Lambda(k)$ curves for et03.dat, where for convenience the evolution time is in units of the mean period of the motion. Similar curves have been found for all other data sets. First, we observe that for small k, there exists no linearly increasing parts of the $\Lambda(k)$ curves. Secondly, the $\Lambda(k)$ curves for small k do not collapse together to form a linear envelope. The above two statements may be made more quantitative as follows. First, for the small k segment of each $\Lambda(k)$ curve, one fits a linear regression line. Then one estimates how the actual $\Lambda(k)$ curves deviate from the fitted straight lines, and how different the slopes of the fitted straight lines are. In any sense, we can safely conclude that there is no evidence of deterministic chaos in the tremor data. This conclusion was also inferred by Timmer et al. (2000). Next, we notice that $\Lambda(k)$ is still not flat for k as large as several tens of the mean period of the motion. This is evident if one compares the $\Lambda(k)$ curves for large k with a constant horizontal line. Hence, we conclude that even the (unrealistic) clean pathological tremor dynamics is not chaotic.

The nonflatness of the $\Lambda(k)$ curves in Fig. 3 for large k is an indication that the underlying dynamics of the tremor oscillation is a diffusional process. To study properties of diffusional processes, we compute the logarithmic displacement curves. They are obtained by rewriting (3) as (Gao 1997)

$$D(k) = \langle \ln \|X_{i+k} - X_{j+k}\| \rangle = \langle \ln \|X_i - X_j\| \rangle + \Lambda(k) \ , \tag{4}$$

and plotting $\langle \ln \|X_{i+k} - X_{j+k}\| \rangle$ as a function of the evolution time k. For the stochastically driven van der Pol oscillator, we have observed that for large k, $\langle \ln \|X_{i+k} - X_{j+k}\| \rangle \sim \ln k^{\alpha}$, with $\alpha = 1/2$ (Gao 1997). In obtaining the exponent α, we used an awkward procedure by fitting the curve $\langle \ln \|X_{i+k} - X_{j+k}\| \rangle$ versus k. With that method, while the estimation of α could still be accurate, the determination of the scaling region is problematic.

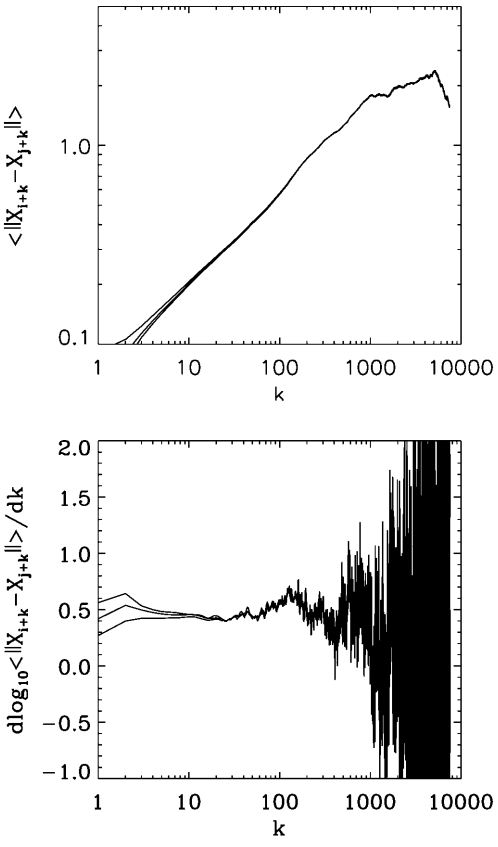

Fig. 4. **a** Log–log plot of the displacement curves for a 3 dimensional random walk. **b** The local slopes. The three curves, from *top* to *bottom*, correspond to shells $(2^{-(i+1)/2}, 2^{-i/2})$ with $i = 9$, 10, and 11. The unit for the evolution time k is simply the sampling points. 30 000 points were used in the computation

One may wish to use local slopes to establish the scaling law and estimate the diffusion exponent α. To check how useful this idea is, we consider a standard Brownian motion, $y(n) = \sum_{i=1}^{n} x(i)$, where $x(i)$ are independent and identically distributed Gaussian noise with mean zero and a standard deviation of one. It is easy to show that $\langle y(n)^2 \rangle = n$, and $\langle y(n)^4 \rangle = 3n^2$, where the angle brackets denote ensemble averages. We embed $y(n)$ time series to 3-D to obtain a 3-D random walk. Figure 4a shows the $\langle \|X_{i+k} - X_{j+k}\| \rangle$ versus k curve on a log–log scale. We observe the curve to be linear up to around 1000 sampling points. (After $k \geq 1000$, the scaling breaks down, due to finiteness of the data set.) Figure 4b shows the local slopes. We do not observe any good plateau, especially for $k \geq 50$. The underlying reason for this behavior is that each point on the curve is proportional to $\ln n^{1/2}$, as is the deviation of each point. Hence, in a local slope plot, we observe small fluctuations (around the plateau) for small n, and large fluc-

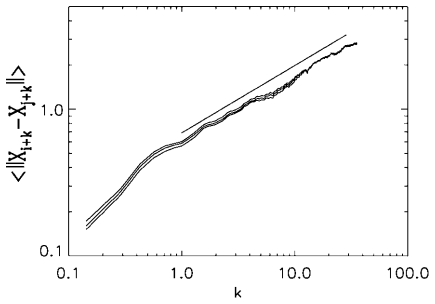

Fig. 5. Log–log plot of the displacement curves for the stochastic van der Pol oscillator. The three curves, from *top* to *bottom*, correspond to shells $(2^{-(i+1)/2}, 2^{-i/2})$ with $i = 9$, 10, and 11. The unit for the evolution time k is the mean period of the motion, which is 211 sampling points and hence comparable to the tremor data. A *straight line*, obtained by linear least-squares fitting the corresponding portion of the curve, is also shown. 30 000 points were used in the computation

tuations for large n. This is a characteristic of diffusional processes. Because of this feature, even the modified approach – i.e., smoothing the logarithmic displacement curve using moving averages before taking the local slopes – will not work as desired for reasonably large n.

Based on the above considerations, we shall not pursue the idea of local slopes further in this study. Instead, we use the following primitive approach to establish the scaling law and estimate the diffusion exponent. We plot $\langle \|X_{i+k} - X_{j+k}\| \rangle$ versus k on a log–log scale, identify a scaling region visually, then estimate α from the slope of the linear portion of the curve. When a region extends over at least several oscillation periods, we say the region may be qualified as a scaling regime; otherwise, it is not. Whenever a knee point can be easily identified from the log–log plot of $\langle \|X_{i+k} - X_{j+k}\| \rangle$ versus k curves, and the portion before and beyond the knee point appears quite straight and extends several oscillation periods long, we then take that as multiple scaling. With this slightly modified procedure (as compared to the one used in Gao 1997 and Gao et al. 1999c), we have re-examined the stochastic van der Pol oscillator. The result is plotted in Fig. 5. Again, for convenience, the evolution time k is in units of the mean period of the oscillation. The straight line is a linear least-squares fit of the corresponding portion of the curve. We find that the slope of the straight line is 0.46. While this number is slightly smaller than 0.5, they are quite close.

We note in Fig. 5 that the three curves separate from each other for k values up to about one mean period of the oscillation. This manifests that the system retains a memory of which shell the curves originate from. When the displacement curves are computed on a series of balls instead of a series of shells, such a feature will be less obvious. We suggest that the scaling region for the diffusion starts from where the memory is lost. Note that for true chaotic systems, the time scale for such memory, i.e., k_p, would typically be considerably shorter than one mean period of the oscillation.

When a phase point near the underlying deterministic limit cycle is kicked farther and farther off the attractor, the convergent flow toward the attractor becomes stronger. Eventually the convergent flow would be so strong that effectively no further separation occurs. This means that the diffusional scaling law will no longer be valid after $k > K_d$, where K_d is some suitable time scale for the diffusional scaling law to be valid. Since K_d depends on the features of the vector field, it is system dependent. For the stochastic van der Pol oscillator (Fig. 5), we observe that $K_d \sim 30T$, where T is the mean oscillation period. We shall see later that K_d is typically several tens of the mean oscillation period for the pathological tremor data. Since it is sensible to assume that an experimental time series is usually on the order of $100T$ long, K_d is typically a significant fraction of the total length of the time series.

Displacement curves have been computed for all the tremor data sets. Good scalings have been observed in all the cases, indicating that pathological tremors behave as diffusional processes. Sometimes we even observe two distinct scaling regimes. Examples are shown in Fig. 6 for et01.dat, et03.dat, et05.dat, park01.dat, park04.dat, and park05.dat. In the figure, straight lines obtained by linear least-squares fitting of the corresponding displacement curves are also shown, to indicate the scaling regime(s). The scaling exponents α, together with their scaling regime, are listed in Tables 1 and 2. For a data set with a single scaling regime, the second exponent and its scaling regime are then left blank in Tables 1 and 2. Note that for simplicity, we have disregarded the possibility that the data points used for the linear regression may not be independent, and instead used the standard formulae to estimate the error of the diffusion coefficient. Such a formulae can be found, for example, in Gordon and Gordon (1994).

To briefly summarize, we have demonstrated that pathological tremors behave as diffusional processes for time scales from about one to several tens of the mean oscillation period. Sometimes we even observe two scalings in this time-scale range. The mechanism for two scalings is, however, still unknown. The diffusion time scale is in sharp contrast to the short-term predictable time scale of chaos, which is typically only a small fraction of the mean oscillation period (for example, up to 0.1–$0.2T$ was studied in Timmer et al. 2000). When the short time scale is not interesting, further analysis of diffusional behavior – provided that the length of the total time series is on the order of 100 mean oscillation periods – is highly recommended.

Next we turn to a discussion on characterizing quantitatively certain aspects of the variations in the pathological tremors. Firstly we note that though qualitatively the pathological tremor data show certain similarity to that of the stochastic van der Pol oscillator (Timmer et al. 2000), quantitatively they can be very different. This difference is characterized by the values of the exponent. In Gao et al. (1999b,c) and Hwang et al. (2000), we have argued that when the value of the diffusion exponent α is larger than 0.5, the diffusion is anomalous. Thus all the tremor data, except for the first scaling regime of et03.dat, park04.dat, and park05.dat, belong to this category. The anomalous diffusion in pathological tremors may indicate that the parameters

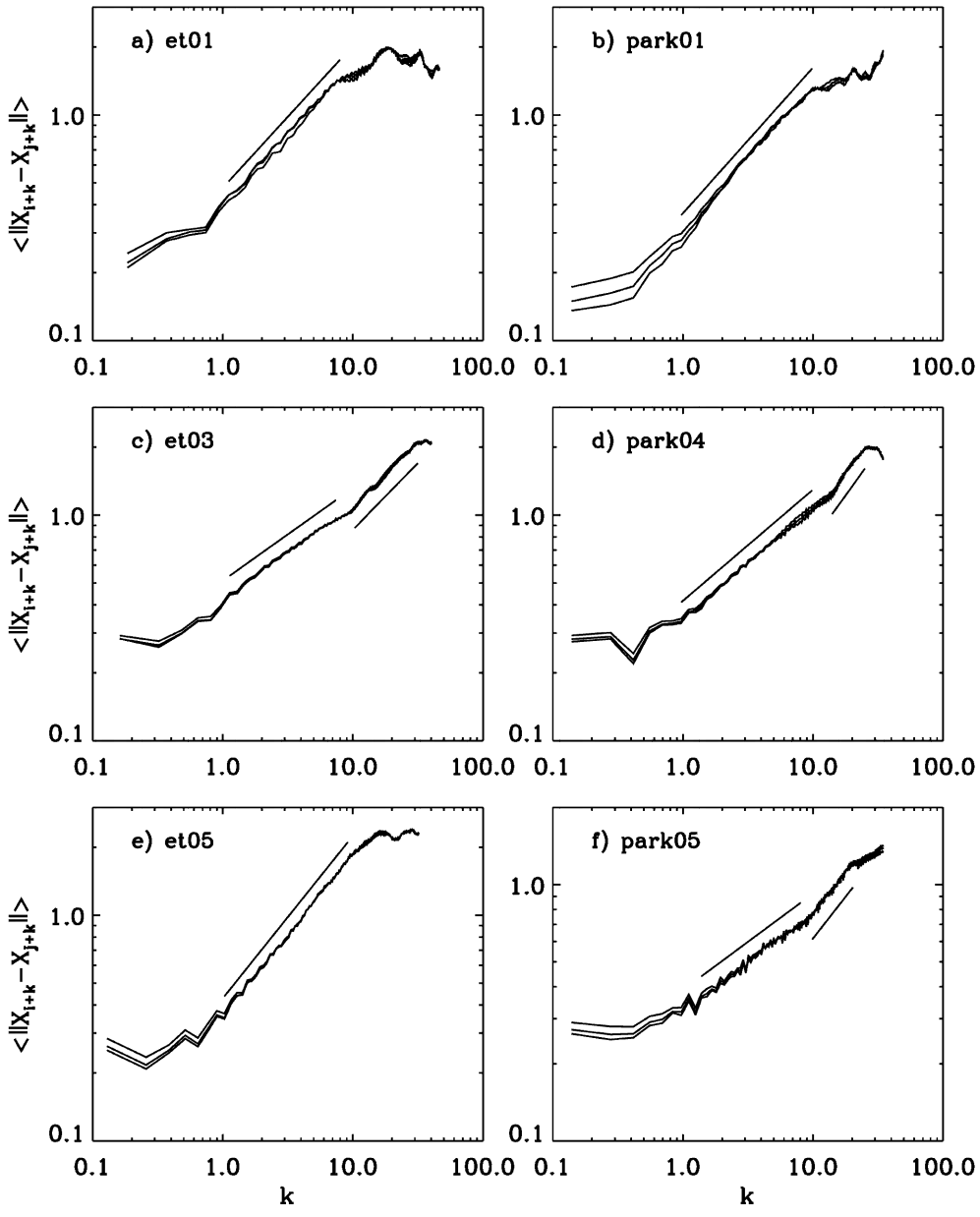

Fig. 6a–f. Same as the caption of Fig. 5, except relating to the tremor data

for tremor oscillators could be quite close to some bifurcation points, hence the convergent flow to the underlying deterministic limit cycle could be very weak. If this is the case, then at the right parameter values and noise level it may be possible to observe noise-induced chaos (Gao et al. 1999b,c; Hwang et al. 2000).

We note that the primary purpose of Timmer et al. (2000) was not in modeling pathologic tremors by the van der Pol oscillator, but in exploring how stochasticity may play some role in tremor dynamics. Now we see that in terms of chaos theory, the stochastic van der Pol oscillator is also quite different from pathological tremors.

At this point, we also note that the stochastic van der Pol oscillator shows higher harmonics in the spectrum at $3, 5, \ldots$ multiples of the fundamental frequency, while the pathological tremors show them at the $2, 3, 4, \ldots$ multiples. Hence, the stochastic van der Pol oscillator is not a good model for pathological tremors, even in terms of spectral analysis.

Secondly, we calculate a simple and useful geometrical quantity for characterizing a diffusional process: the diffusion width, $\mathrm{DIFFU}_{\mathrm{width}}$. This is estimated as follows (Gao 1997): In a 2-D embedding space, isolate a small portion of the diffused limit cycle, $\{x(t) : x(t) > 0, |x(t+L) - x(t)| < \epsilon\}$, where ϵ is a positive number that can be chosen more or less arbitrarily so long as it is small. Such a region is schematically shown as a narrow box in Fig. 2 in dashed lines. From this subdata set, we compute the mean and the standard deviation. We then estimate $\mathrm{DIFFU}_{\mathrm{width}}$ from the ratio of the standard deviation and the mean. For a specific system, $\mathrm{DIFFU}_{\mathrm{width}}$ monotonically increases with the noise level $\eta(t)$. However, for different systems, even with the same amount of noise, $\mathrm{DIFFU}_{\mathrm{width}}$ can have wide variations. For example, when the convergent flow to the underly-

ing deterministic limit cycle is weak, then $\mathrm{DIFFU}_{\mathrm{width}}$ can be quite large even the noise is very weak (Gao et al. 1999b). We thus anticipate $\mathrm{DIFFU}_{\mathrm{width}}$ to have wide variations among the pathological tremor data sets, since different patients should be expected to have different effective noise levels, and the parameters for the underlying nonlinear oscillators should also be expected to have wide variations among the patients. Indeed, we observe from Tables 1 and 2 that $\mathrm{DIFFU}_{\mathrm{width}}$ varies widely among the patients.

A 1-D version of $\mathrm{DIFFU}_{\mathrm{width}}$ can be obtained as follows. In each period of the oscillation, obtain the maxima of the signal to form an estimate of the amplitude of the oscillation. Then compute the mean and standard deviation of the amplitudes, and form their ratio, $\sigma(A)/\bar{A}$. Denote this quantity by $\mathrm{AMP}_{\mathrm{fluc}}$. Indeed, we see from Tables 1 and 2 that the values of $\mathrm{AMP}_{\mathrm{fluc}}$ are quite close (sometimes even identical) to $\mathrm{DIFFU}_{\mathrm{width}}$. This should not be surprising, since the dashed box indicated in Fig. 2 contains mainly the positive acceleration peaks, which are closely related to $\mathrm{AMP}_{\mathrm{fluc}}$.

4 Discussion and conclusions

We have studied two types of pathological tremors, essential and Parkinsonian, using dynamical systems theory. We have shown that pathological tremors can be characterized as diffusional processes. The time-scale range for the diffusional scaling law to be valid starts from about one to several tens of the mean oscillation period. This time-scale range contrasts sharply with the predictable time scale for deterministic chaos, which is usually only a small fraction of the mean oscillation period. The diffusions in pathological tremors are usually anomalous.

Disappointed at being unable to discriminate between essential and Parkinsonian tremors, Timmer et al. (2000) surmised that there might be more similarities than substantial differences between the two pathological processes. The similarities come from the fact that both types of tremors are diffusional processes, and hence they belong to the same dynamical class. Indeed, although we have designed many parameters such as the diffusion exponents and their scaling regions, the diffusion width, and the fluctuation of the amplitude to characterize a diffusional process, the values of these parameters do not appear to form good basis for discriminating between Parkinsonian and essential tremors. On the contrary, they indicate many similarities between these two types of tremors.

The above discussion has an interesting and important implication. That is, when searching for quantities that might be able to discriminate between different pathological tremors, those quantities better not be purely of dynamical origin, since quantities that are purely of dynamical origin characterize more the similarities than the differences between different pathological tremors. Indeed, we have seen that the nondynamical quantity L/T, which is the ratio between the embedding delay time and the mean oscillation period, is a much more promising quantity in discriminating between essential and Parkinsonian tremors (Tables 1 and 2).

The present work has created more questions than it has answered. For example, we can ask: What are the origins of the anomalous diffusions in pathological tremors? Why are there multiple scalings? Might the dynamical quantities, such as the noise level, the diffusion exponents, the diffusion width, and the fluctuation of the amplitude, change in the course of medical treatment? If the answer is yes, we can further ask: Will these changes provide useful information to the treatment of pathological tremors? These questions are posed here with the hope that they may stimulate researchers in the field to design new experiments in the future.

Acknowledgements. The authors thank Dr. Alessandro Giuliani for directing their attention to the work of Timmer et al., and Dr. Jens Timmer for providing them with the tremor data analyzed here, and for some useful discussions.

References

Bock O, Wenderoth N (1999) Dependence of peripheral tremor on mechanical perturbations: a modeling study. Biol Cybern 80: 103–108

Deuschl G, Bain P, Brin M (1998) Consensus statement of the movement Disorder Society on Tremor. Mov Disord 13 [Suppl 3]: 2–23

Elble RJ, Koller WC (1990) Tremor. Johns Hopkins University Press, Baltimore, md

Gao JB (1997) Recognizing randomness in a time series. Physica D 106: 49–56

Gao JB, Zheng ZM (1993) Local exponential divergence plot and optimal embedding of a chaotic time series. Phys Lett A 181: 153–158

Gao JB, Zheng ZM (1994a) Direct dynamical test for deterministic chaos. Europhys Lett 25: 485–490

Gao JB, Zheng ZM (1994b) Direct dynamical test for deterministic chaos and optimal embedding of a chaotic time series. Phys Rev E 49: 3807–3814

Gao JB, Hwang SK, Liu JM (1999a) Effects of intrinsic spontaneous-emission noise on the nonlinear dynamics of an optically injected semiconductor laser. Phys Rev A 59: 1582–1585

Gao JB, Hwang SK, Liu JM (1999b) When can noise induce chaos? Phys Rev Lett 82: 1132–1135

Gao JB, Chen CC, Hwang SK, Liu JM (1999c) Noise-induced chaos. Int J Mod Phys B 13: 3283–3305

Gordon SP, Gordon FS (1994) Contemporary statistics. McGraw-Hill, New York, pp 502–511

Gresty M, Buckwell D (1990) Spectral analysis of tremor: understanding the results. J Neurol Neurosurg Psychiatry 53: 976–981

Hwang SK, Gao JB, Liu JM (2000) Noise-induced chaos in an optically injected semiconductor laser model. Phys Rev E 61: 5162–5170

Kantz H (1994) A robust method to estimate the maximal Lyapunov exponent of a time series. Phys Lett A 185: 77–87

Mannella R, Palleschi V (1989) Fast and precise algorithm for computer simulation of stochastic differential equations. Phys Rev A 40: 3381–3386

Packard NH, Crutchfield JP, Farmer JD, Shaw RS (1980) Geometry from a time series. Phys Rev Lett 45: 712–716

Rosenstein MT, Collins JJ, Deluca CJ (1993) A practical method for calculating largest Lyapunov exponents from small data sets. Physica D 65: 117–134

Rossler OE (1976) An equation for continuous chaos. Phys Lett A 57: 397–398

Takens F (1981) Detecting strange attractors in turbulence. In: Rand DA, Young LS (eds) Dynamical systems and turbulence. (Lecture notes in mathematics, vol 898) Springer, Berlin Heidelberg New York, p 366

Timmer J, Haussler S, Lauk M, Lucking CH (2000) Pathological tremors: deterministic chaos or nonlinear stochastic oscillators? Chaos 10: 278–288

Wenderoth N, Bock O (1999) Load dependence of simulated central tremor. Biol Cybern 80: 285–290